

ROOM TEMPERATURE MAGNETS IN FRIB DRIVER LINAC*

Y. Yamazaki[#], N. Bultman, E. Burkhardt, F. Feyzi, K. Holland, A. Hussain, M. Ikegami, F. Marti, S. Miller, T. Russo, J. Wei, Q. Zhao, Facility for Rare Isotope Beams, Michigan State University, East Lansing, MI 48824, USA
 W. Yang, Q. Yao, Institute of Modern Physics, Lanzhou, China

Abstract

The FRIB Driver Linac is to accelerate all the stable ions beyond 200 MeV/nucleon with a beam power of 400 kW. The linac is unique, being compactly folded twice. In this report, the room temperature magnets, amounting 147 in total, after Front End with a 0.5-MeV RFQ, are detailed, emphasizing the rotating coil field measurements and fiducialization.

INTRODUCTION

The driver linac of the Facility for Rare Isotope Beams (FRIB) [1, 2] is to accelerate all the stable ions (including uranium) up to or beyond 200 MeV/nucleon (MeV/u) with a beam power of 400 kW (5×10^{13} $^{238}\text{U}/\text{s}$). The linac is twice folded as shown in Fig. 1 in order to make it sufficiently compact to be located in the university campus, and to reuse the existing experimental facility. The linac is divided into seven segments; Front End (FE), Linac Segment (LS) 1, Folding Segment (FS) 1, LS2, FS2, LS3, and Beam Delivery Segment (BDS). Figure 1 is also showing the segments where the room temperature (RT) magnets to be reported here are located. The other segments were filled out by accelerating cyomodules (CMs), to which superconducting (SC) solenoids attached with horizontal and vertical dipoles are installed for transverse focusing and steering.

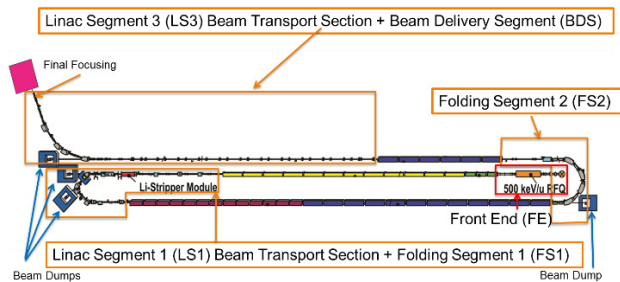


Figure 1: FRIB driver linac showing the segments (boxed in orange) where the RT magnets to be reported here are placed.

Figure 2 shows all the magnets to be used for the FRIB driver linac. The beam transport sections are equipped with the standard quadrupole magnets Q1s and the standard corrector magnets C2s. Most of C2s (44 of 46) are from Lawrence Berkeley National Laboratory (LBNL), being not reported here. A dog leg consisting of four 5-degree dipole D1s is located on each side of the liquid lithium charge stripper in order to protect SC cavi-

*Work supported by the U.S. Department of Energy Office of Science under Cooperative Agreement DE-SC0000661 and the National Science Foundation under Cooperative Agreement PHY-1102511.
[#]yamazaki@frib.msu.edu

ties from any lithium sputtering. In total, 151 RT magnets are completed or under construction by an outside vendor, including 4 spare Q1s to be used for the case of one CM missing. Note that H stands for hexapole (sextupole).

Figure 2: Magnets for the FRIB driver linac.

Originally, it was planned to use combined function magnets of quadrupole and sextupole for FS1 and BDS. After the separate function solution was found [3], all the linac RT magnets become quite common ones. Then, the manufacturing and the testing of these common magnets need no technical challenges. On the other hand, due care is still necessary for these magnets to guide the high power beams to be focused on the target with small emittances and sizes. Also, any project always need good value engineering (separate function rather than combined function was most effective example).

FIELD MAPPING RESULTS

Even if all the magnets have easily obtainable performance, we need to verify that all the magnets have required performance. The field mapping is performed by means of a all probe for one magnet of each type of quadrupoles and sextupoles and for all the dipole magnets. The absolute integrated field measured so far were compared with the requirement in Table 1. All the measurement results with the specified currents exceed the required values.

Table 1: Integrated Fields

Magnet Type	Required	Measured
Q1	$\geq 8.7 \text{ T/m}$	9.5 T/m
Q2	$\geq 7.8 \text{ T/m}$	8.5 T/m
Q6	$\geq 3.0 \text{ T/m}$	3.2 T/m
H3	$\geq 3.0 \text{ T/m}^2$	3.9 T/m
C1	$\geq 0.0060 \text{ T}$	0.0063 T
C3	$\geq 0.0160 \text{ T}$	0.0160 T

Table 2 shows the measured results of field uniformity compared with the modelling and requirements. It can be seen that the measured results are slightly worse than the modelling as expected, but are within the requirements.

Table 2: Integrated Field Uniformity in Good Field Region (% in full)

Magnet Type	Required	Modelled	Measured
Q1	1.0	0.4	0.6 ± 0.1
Q2	1.4	0.4	0.5 ± 0.1
Q6	1.4	1.2	1.1 ± 0.2
H3	10	5.0	4.9 ± 1.0
C1	20	1.4	1.8 ± 0.4
C3	20	2.4	3.0 ± 0.6

ROTATING COIL MEASUREMENTS

The rotating coil measurements [4] were carried out for all the quadrupole and sextupole magnets. The system is comprised of two coils; the main coil and the compensation coil. In the case of quadrupole magnets, the compensation coil output cancels both dipole and quadrupole components of the main coil output, so that the higher multipole ones can be measured with high accuracy.

Figure 3 shows typical results of both the main coil output and the compensated output. The dipole component can be seen from the slight deviation from the periodicity, indicating the field center axis being deviated from the rotating axis.

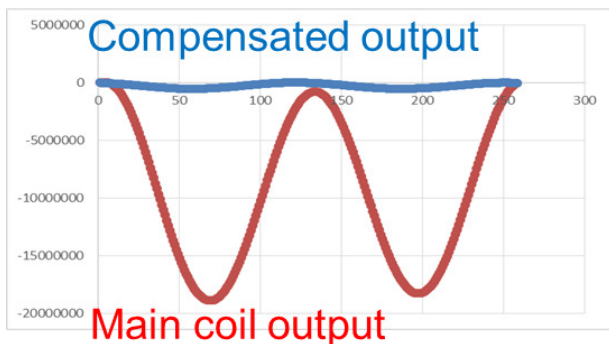


Figure 3: The output signal from the main coil and that compensated by the compensation coil. The coil is rotating at a period of 3 s.

Figure 4 shows the quadrupole component of the main coil output calibrated to the integrated field gradient versus the current. Figure 5 shows the deviation of the field axis from the rotating axis, derived from the dipole component of the main coil output versus the current. The deviation is within 0.1 mm, but the alignment will be done by using these data. Therefore, the alignment error should be significantly improved. Figure 6 shows the higher multipole components (2n-pole) obtained from Fourier analysis of the compensated output. Here, n = 6 is

allowed multipole. The small values are consistent with the uniformity shown in Table 2.

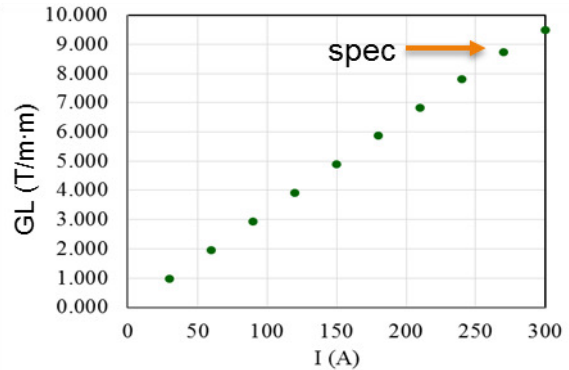


Figure 4: Excitation curve of the first Q1.

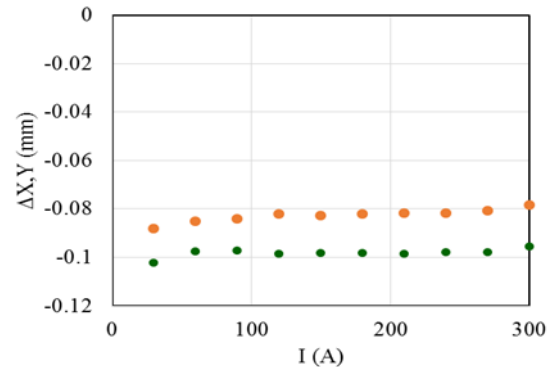


Figure 5: The deviation of the field center from the rotating axis. No significant current dependence observed.

	299.97A
mod(B3/B2)	4.8355E-04
mod(B4/B2)	1.9973E-04
mod(B5/B2)	1.0134E-04
mod(B6/B2)	4.3800E-04
mod(B7/B2)	2.0190E-05
mod(B8/B2)	4.7200E-05
mod(B9/B2)	4.6930E-05
mod(B10/B2)	1.7663E-04
mod(B11/B2)	2.3580E-05
mod(B12/B2)	2.5160E-05
mod(B13/B2)	1.4800E-05
mod(B14/B2)	2.8020E-05
mod(B15/B2)	1.5070E-05
mod(B16/B2)	1.6780E-05
mod(B17/B2)	2.1150E-05
mod(B18/B2)	1.0180E-05
mod(B19/B2)	1.6530E-05
mod(B20/B2)	1.3210E-05

Figure 6: Multipole components obtained from Fourier analysis of the compensated output.

In order to confirm the rotating coil results, the measurement was performed at various rotating speed and different time. Figure 7 verifies the $n = 6$ component independent of rotating velocity. It is interesting to note that the saturation effect is much more prominent in the current dependence of the $n = 6$ component than the quadrupole component, since the $n = 6$ component arises from the non-uniformity at the pole edge.

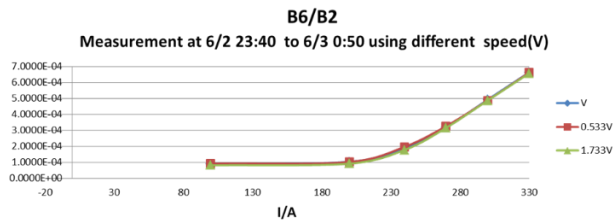


Figure 7: Rotating velocity dependence of excitation curve of $n = 6$ component of the second Q1.

FIDUCIALIZATION AND ALIGNMENT

Six fiducials are used for each magnet in order to ensure four fiducials redundantly observable from any directions. To all the magnets, six hexagon shaped fiducial fixtures (Figure 8 a)) are lightly welded. A $\frac{1}{4}$ " shank pin nest (Figure 8 b)) is inserted into each fixture, and the $\frac{1}{2}$ " spherical mirror reflector (SMR) used for a laser tracker is attached to the shank pin nest as shown in Figure 8c). The same system is used for the field measurement and the alignment.



Figure 8: From left to right, a) fiducial fixtures, b) $\frac{1}{4}$ " shank pin nest, and c) $\frac{1}{2}$ " SMR.

For fiducialization, the coordinate system is established by measuring the coordinates of four pole gap centers on each end (quadrupole case) by means of the laser tracker. With respect to the system thus established, the coordinates of the six fiducials are measured by putting the SMR into the nest for the laser tracker. The rotating coil system with a cylindrical shell just fitted to a magnet aperture is inserted into the magnet aperture, being approximately located at the mechanical central axis. Then, the rotating axis of the rotating coil system was measured with respect to the above coordinate system by means of the laser tracker. The spatial relation between the rotating axis and fiducials thus measured is captured into a laser tracker software which is common between the fiducialization and alignment. The field-measured data exemplified by Figure 5 shall be taken into account for the magnet alignment.

CONCLUSION

Among the 151 FRIB driver linac RT magnets ordered to the outside vendor, 128 were completed to date, and it is forecasted that all are to be completed towards the end of 2016. The FRIB effort has been devoted to the value engineering, finding the possible design of the separate function to replace the combined function quadrupole and sextupole and using the rotating coil to ensure the performance of all the magnets. All the 128 completed magnets passed the excitation tests, the rotating coil measurement tests or hall probe mapping tests.

ACKNOWLEDGMENT

We would like to express our thanks to FRIB and NSCL members and FRIB collaborators for their supports.

REFERENCES

- [1] J. Wei *et al*, HIAT'12, 8 (2012); 417 (2012); NA-PAC'13, 1453 (2013); HB'14, 12 (2014).
- [2] Y. Yamazaki *et al*, IPAC'15, 4051 (2015); IPAC'16, 2039 (2016).
- [3] Y. Yamazaki *et al*, LINAC'14, 532 (2014).
- [4] J. Tanabe, "Iron Dominated Electromagnets Design, Fabrication, Assembly and Measurements", SLAC-R-754 (2005), and many others.